

## Monitoring ground improvement using in situ tests in Guayaquil, Ecuador

### Author 1

- Daniel Falquez, Eng.
- Department of Earth Sciences, Escuela Superior Politécnica del Litoral, Guayaquil, Ecuador
- <https://orcid.org/0000-0001-8779-1930>

### Author 2

- Francisco Ripalda Zenck, Eng.
- Department of Earth Sciences, Escuela Superior Politécnica del Litoral, Guayaquil, Ecuador
- <https://orcid.org/0000-0001-9756-1493>

### Author 3

- Davide Besenon, MSc.
- Department of Earth Sciences, Escuela Superior Politécnica del Litoral, Guayaquil, Ecuador
- <https://orcid.org/0000-0002-3384-3747>

### Author 4

- Roberto Luque Nuques, PhD
- Department of Earth Sciences, Escuela Superior Politécnica del Litoral, Guayaquil, Ecuador
- Geosísmica, Guayaquil, Ecuador

### Author 5

- Fernando Illingworth, MSc.
- Subterra, Guayaquil, Ecuador

### Author 6

- Sara Amoroso, PhD.
- University of Chieti-Pescara, Pescara, Italy
- Istituto Nazionale di Geofisica e Vulcanologia, Italy
- <https://orcid.org/0000-0001-5835-079X>

## Abstract

This paper describes the use of the seismic dilatometer test (SDMT) and the piezocone test (CPTu), to assess the effects of ground improvement in preventing liquefaction damage at a wastewater treatment plant in Guayaquil, Ecuador. The ground improvement consisted of 15 m-long, 0.55 m-diameter and 2 m-spacing stone columns built with vibro-replacement technique. The tests were carried out both in natural and in treated soils, in order to compare the variation of the geotechnical parameters in the analyzed deposits, also combining DMT and CPTu results in sandy deposits to estimate the overconsolidation ratio (OCR), the at-rest lateral earth pressure coefficient ( $K_0$ ) and the ratio between the constrained modulus and the corrected cone resistance ( $M/q_c$ ). Due to the presence of liquefiable soils at the trial site, the test results were then used to evaluate the pre and post-treatment liquefaction severity indexes, using different methods based on CPT, DMT, combined CPT-DMT, and shear wave velocity ( $V_s$ ) approaches for a design ground motion. The results show a certain

sensitivity of the DMT over the CPTu tests to the ground improvement into the layer composed by sands and sandy silts, while  $V_s$  values show a limited increase in the treated area.

## Keywords

Ground improvement, liquefaction, in situ testing

## List of notations

$FC$	is the fines content of the soil
$PI$	is the plasticity index of the soil
$SC$	is stone column
$I_i$	is the improvement index
$NS$	is natural soil (before the installation of the SC)
$TS$	is the treated soil (after the installation of the SC)
$GWT$	is the ground water table
$\sigma'_{v0}$	is the vertical effective stress
$u_0$	is the equilibrium pore water pressure
$N_{SPT}$	is the SPT blow count
$(N_1)_{60}$	is the SPT corrected penetration resistance
$(N_1)_{60,cs}$	is the equivalent clean-sand corrected standard penetration resistance
$q_c$	is the cone resistance
$q_t$	is the corrected cone resistance for pore water pressure in cohesive soil
$q_{c1}$	is the corrected cone resistance for overburden stress
$q_{c1N}$	is the normalized corrected cone resistance for overburden stress
$(q_{c1N})_{cs}$	is the equivalent clean-sand normalized cone resistance (CPTu)
$I_c$	is the soil behavior index
$D_R$	is the relative density
$\varphi'$	is the effective friction angle
$I_D$	is the material index
$K_D$	is the horizontal stress index
$K_0$	at-rest lateral earth pressure coefficient
$OCR$	is the overconsolidation ratio
$M$	is the constrained modulus
$V_s$	is the shear wave velocity
$V_{s1}$	is the corrected shear wave velocity ( $V_s$ )
$M_w$	is the moment magnitude
$MSF$	is the magnitude scaling factor
$PGA$	is the peak ground acceleration
$r_d$	is the shear stress reduction coefficient
$CSR_{M=7.5}$	is the cyclic stress ratio at 7.5 moment magnitude

$CRR_{M=7.5}$  is the cyclic resistance ratio at 7.5 magnitude

$FS_{LIQ}$  is the factor of safety to liquefaction

$LPI$  is the liquefaction potential index

$H_1$  is the non-liquefiable capping layer

$LPI_{ISH}$  is the Ishihara-inspired liquefaction potential index

$\epsilon_v$  is the post-liquefaction volumetric strain

$LSN$  is the liquefaction severity number

$S$  is the liquefaction-induced vertical settlement

## 1. Introduction

Ground improvement is a field that involves different techniques to modify the soil response under different conditions. The decision regarding ground modification performance is based on the assessment of difficult soils, liquefaction potential, soil instability, insufficient bearing capacity and/or excessive settlement, seepage (U.S. Army Corps of Engineers, 1999).

In particular, liquefaction is the soil response to the loss of stiffness and strength due to pore pressure increment, reducing the effective stress. This increment is caused by an elevation of the hydraulic gradient or through dynamic loading of the soil (Knappett and Craig, 2012). A form to mitigate the liquefaction potential is through densification of the soil by the following treatments: deep dynamic compaction, vibro-compaction, blasting and vibro-replacement (Mitchell, 1981; U.S. Army Corps of Engineers, 1999; Shenthan *et al.*, 2004; Mackiewicz and Camp, 2007). The characteristics of the soil, such as gradation and density, project requirements, limitation of space, adjacent structures and ground water table, are aspects to consider for selecting the appropriate treatment. Mitchell (2008) discussed the applications and limitations of these densification methods, noting that the degree of improvement given by the deep dynamic compaction, vibro-compaction and blasting is greater in clean sands and decreases as the fines content (FC) increases. Nevertheless, several studies document mitigation works using a variety of FC values (including rather elevated percentages) highlighting an increase of improvement given by the vibro-replacement stone columns: Mackiewicz and Camp (2007) used an improvement index ( $I_i$ ), given by the ratio between the cone resistance ( $q_c$ ) after and before the treatment minus one, to provide an improvement of  $0.3 < I_i < 2.8$  for  $FC < 5\%$ , and of  $0 < I_i < 1.6$  for  $15\% < FC < 40\%$ ; Luehring *et al.* (2001) showed an increase of 95% for the corrected SPT blow count  $(N_1)_{60}$ , and of 180% for the normalized corrected cone resistance  $q_{c1N}$ , using vibro-replacement stone columns in combination with vertical drains in deposits with  $FC < 65\%$ . Mitchell and Wentz (1991) showed an average 100% increase for the corrected cone resistance for overburden stress ( $q_{c1}$ ) and an average 45% increase for the SPT corrected penetration resistance,  $(N_1)_{60}$ , when comparing pre and post treatment results in soil layers with  $FC < 55\%$ . Vibro-replacement stone columns installation may have the double beneficial effect to cause densification of the surrounding soil during installation and to facilitate the dissipation of the excess of pore water pressure developed during an earthquake, by providing a shorter path of drainage (Adalier and Elgamal, 2004).

Therefore, it results of interest to verify the effectiveness of the improvement using in situ tests. These tests allow for developing a quick assessment, which consists in the comparison of selected geotechnical parameters obtained before and after the treatment. Currently, there is a wide selection of in situ tests.

32 Depending on the location, the availability of specific in-situ testing equipment is also a factor to consider in  
33 evaluating the ground improvement. Numerous authors (Schmertmann, 1986; Mackiewicz and Camp, 2007;  
34 Mitchell, 2008; Monaco *et al.*, 2014; Bałachowski and Kurek, 2015; Amoroso *et al.*, 2018, 2020; Massarsch  
35 and Fellenius, 2019; Massarsch *et al.*, 2020) evaluate the change of the soil characteristics achieved, using at  
36 least one of the following tests and their parameters: SPT blow count  $N_{SPT}$  in the standard penetration test  
37 (SPT), horizontal stress index  $K_D$  and constrained modulus  $M$  in the flat dilatometer test (DMT), corrected cone  
38 resistance  $q_t$  in the piezocone penetrometer test (CPTu), and shear wave velocity  $V_s$  in the geophysical  
39 measurements provided by invasive or non-invasive tests (e.g. seismic piezocone SCPTu, seismic dilatometer  
40 SDMT, down-hole DH, cross-hole CH, multichannel analysis of surface waves MASW). Moreover, several  
41 studies discuss the change in the at-rest lateral earth pressure coefficient  $K_0$ , the overconsolidation ratio OCR  
42 and the ratio  $M/q_t$  when monitoring the densification effectiveness and the lateral stress increase. To estimate  
43 the parameters mentioned above, a combination of CPT and DMT tests is performed, as suggested in previous  
44 studies (e.g. Baldi *et al.*, 1986; Marchetti *et al.*, 2001; Massarsch *et al.*, 2020).

45 Therefore, the present study describes the effects of ground improvement using the seismic dilatometer test  
46 (SDMT) and the piezocone test (CPTu). The location of the trial site is a project site for a wastewater treatment  
47 plant located in a sector known as “Las Esclusas” in Guayaquil, Ecuador. Ground improvement, realized in  
48 different zones of the facility, consisted of 15 m-long, 0.55 m-diameter and 2 m-spacing stone columns built  
49 with the vibro-replacement technique to mitigate the liquefaction potential (Luque, 2018). In this respect, CPTu,  
50 DMT, combined CPTu-DMT parameters and  $V_s$  measurements were executed in natural and treated soils and  
51 the results were compared. Moreover, liquefaction analyses were carried out to verify the column effectiveness  
52 in this key aspect.

## 53 **2. Combination of SDMT and CPTu for monitoring ground improvement**

54 Single-parameters derived separately from SDMT and CPT tests can be used to detect the modification in soil  
55 characteristics due to improvement works. As stated by various authors (e.g. Schmertmann, 1986;  
56 Bałachowski and Kurek, 2015; Amoroso *et al.*, 2018, 2020; Massarsch and Fellenius, 2019; Massarsch *et al.*,  
57 2020), these parameters can be identified in the horizontal stress index  $K_D$  and the constrained modulus  $M$   
58 from DMT, the corrected cone resistance  $q_t$  (or the cone resistance  $q_c$ ) and the relative density  $D_R$  from CPT.  
59  $K_D$  is directly derived from the corrected DMT membrane lift-off pressure reading and contains information  
60 about the stress history of the soil, while  $M$  is a function of the three DMT intermediate parameters (horizontal  
61 stress index  $K_D$ , dilatometer modulus  $E_D$  and material index  $I_D$ ), representing a working strain modulus, i.e. the  
62 modulus that, when introduced into the linear elasticity formulae, provides realistic estimates of the settlement

63 of a shallow foundation under working loads (Marchetti, 1980, 2008; Marchetti *et al.*, 2001). Parameter  $q_t$  (or  
64  $q_c$ ) is a direct measurement from CPT while  $D_R$  is usually based on correlations as function of the cone  
65 resistance and effective stress (Juang *et al.*, 1996). According to previous ground improvement studies related  
66 to densification techniques (e.g. Massarsch and Fellenius, 2002, 2019; Massarsch *et al.*, 2019), the horizontal  
67 stress tends to increase after compaction making  $K_D$  (and therefore  $M$ ) more sensitive than  $q_t$  (and  
68 consequently  $D_R$ ) to detect the modifications induced in by the treatment.

69 Moreover, CPT-DMT parameters can help to identify the effectiveness of the treatment, such as at-rest earth  
70 pressure coefficient  $K_0$ , overconsolidation ratio OCR, and ratio  $M/q_t$  (or  $M/q_c$ ). Ground improvement techniques  
71 by compaction are usually installed in sandy soils with low FC, in order to monitor the effectiveness of the  
72 treatment through  $K_0$  and OCR, the combination of DMT and CPT parameters is used. With reference to  $K_0$  in  
73 sands Baldi *et al.* (1986) and later Hossain and Andrus (2016) developed correlations, mostly derived from  
74 calibration chamber (CC) tests. The present research estimated  $K_0$  using the relationship proposed by Hossain  
75 and Andrus (2016), based on OCR,  $K_D$  and  $q_c/\sigma'_{v0}$ :

$$1. \quad K_0 = 0.72 + 0.456 \log OCR + 0.035 K_D - 0.194 \log q_c / \sigma'_{v0}$$

76 To estimate OCR in sands Marchetti *et al.* (2001) proposed to use the ratio  $M/q_c$  ( $M/q_t \approx 5-10$  in NC sands,  $M/q_t$   
77  $\approx 12-24$  in OC sands) considering the results of DMT and CPT tests performed in compaction works of a sand  
78 fill (Jendeby, 1992), CC tests (Baldi *et al.*, 1988), quality control of ground improvement (Schmertmann *et al.*,  
79 1986). Later, Monaco *et al.* (2014) carried out a field experiment constructing a temporary embankment that  
80 allowed to directly measure the OCR and to correlate it with the ratio  $M/q_t$ :

$$2. \quad OCR = 0.0344 \left( \frac{M}{q_t} \right)^2 - 0.4174 \left( \frac{M}{q_t} \right) + 2.2914$$

81 Schmertmann (1985) highlighted the importance of measuring the soil lateral stress in different scenarios,  
82 remarking that the possible  $K_0$  increment, due to compaction induced effects, depends on the initial  $K_0$  soil  
83 condition. Lateral stress estimations obtained in a test area with an initial high  $K_0$  ( $\approx 1.3$ ) increased merely 3%  
84 after the dynamic compaction, while a much greater increase occurred when natural conditions were  
85 associated to relatively low  $K_0$  ( $\approx 0.6$ ), reaching an increase of 77% after the treatment.

86 The increment of the lateral stress can be also observed by vibratory compaction, as provided by Massarsch  
87 and Fellenius (2002) and Rayamajhi *et al.* (2016). In addition to CPT and SPT tests for the verification of the  
88 performance of the soil improvement, Baez (1995) suggested DMT tests as an important tool to validate the  
89 increase of the lateral stress.  $K_0$  variation is used as an indicator of the treatment effectiveness in sandy

90 deposits (Amoroso *et al.*, 2018; Massarsch *et al.*, 2020), combining DMT and CPT data as detailed above.  
91 Mayne and Kulhawy (1982) and Schmertmann (1985) agreed that OCR depends on  $K_0$ , and therefore OCR is  
92 also a good indicator of the modified effectiveness. Moreover, Massarsch and Fellenius (2019) evaluated the  
93 effects of vibratory compaction concluding that densification produces pre-consolidation effect of the soil  
94 causing an increment in OCR. OCR variation has been observed in several research works: Bałachowski and  
95 Kurek (2015) reported an OCR increase of 100-125% into a sandy deposits due to vibro-flotation while the  
96 ratio  $M/q_c$  increased from 120 to 160%; Kurek and Bałachowski (2015) detected an improvement between 50  
97 and 100% in OCR, while the ratio  $M/q_c$  showed a slight increase due to heavy compaction works in sands with  
98  $FC < 6\%$ ; Amoroso *et al.* (2018) monitored different techniques of improvement and the change in OCR and  
99  $K_0$  profiles was not clearly noticeable possibly due to the compaction technique used and/or the soil variability.  
100 Extensive literature reports that  $M$  increases at a faster rate than  $q_t$ . Therefore, the ratio  $M/q_t$  is often used as  
101 a treatment quality control criterion as it contains also information about the stress history of the soil. (Lee *et*  
102 *al.*, 2011) performed several CC tests finding a higher sensitivity of DMT to the changes of stress history over  
103 CPT, due to the lower soil disturbance of the wedge during its insertion in comparison with the cone.  
104 Consequently, this produces a higher increase of  $K_D$  and subsequently of  $M$  values with respect to  $q_t$   
105 measurements. Therefore, the  $M/q_t$  ratio is also a good indicator of the ground improvement work.

### 106 3. Trial site

107 The trial site was located in Guayaquil (Ecuador) within a wastewater treatment plant (WTP) construction  
108 project close to the banks of the Guayas river in a sector known as “Las Esclusas” as can be observed in  
109 Figure 1(a). The new WTP will treat wastewater generated in the center and south areas of the city. Due to  
110 the low soil properties of some areas of the site, stone columns (SC) were realized in 2018 to support shallow  
111 foundations of different structures, internal roads and to mitigate consolidation settlement of clayey materials  
112 and liquefaction potential of sands and sandy silts (Luque, 2018).

#### 113 3.1. In situ tests

114 Extensive geotechnical investigation was carried out at different stages: design stage (2014), start of  
115 construction works (2017), construction stage (2018), research studies (2019-2020). Field testing included:  
116 boreholes, SPT, CPTu, SDMT, MASW and REMI. The results presented in this study are referred to a trial site  
117 located nearby a clarifier as shown in Figure 1(b), where CPTu and SDMT tests were performed between 2019  
118 and 2020 in natural (NS) and in treated (TS) soil up to 16-20 m depth. NS soil testing are identified as  
119 CPTu1\_NS and SDMT1\_NS, while surveys after SC installation are detected as CPTu2\_TS and SDMT2\_TS.  
120 Additional information regarding the NS condition were obtained from borehole and SPTs (SPTP3\_NS) and  
121 CPTu test (CPTu14\_NS) performed during the WTP construction (Figure 1(b)).

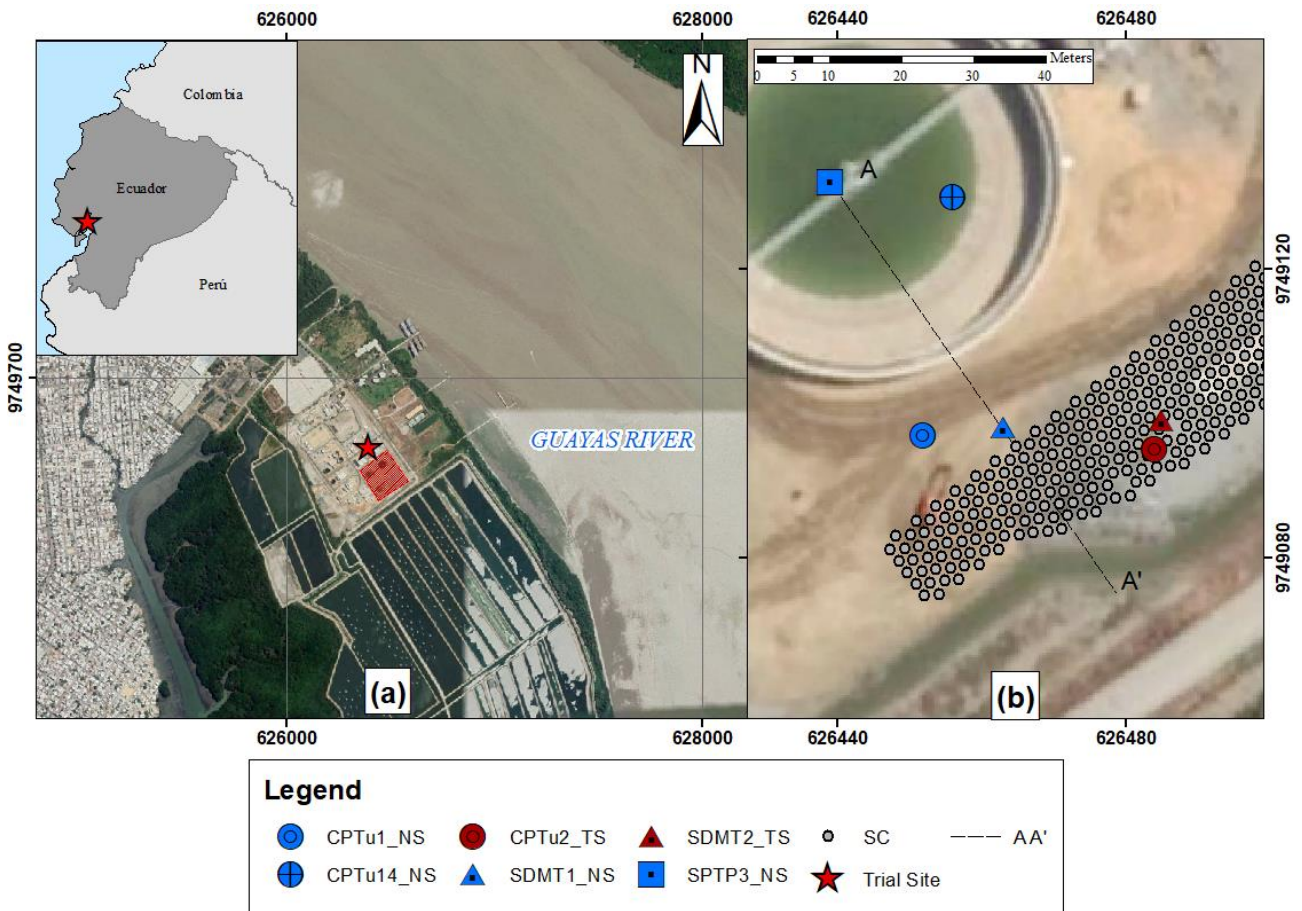


Figure 1. (a) Location of the wastewater treatment plant. (b) Location of in-situ tests and SCs

123

124

125

126

127

128

129

130

131

132

For the execution of CPTus and SDMTs the shallow compacted fill layer ( $\approx 0.6-0.8$  m thick) was removed, to prevent damage on the geotechnical equipment. Collected data was used to define a subsoil model of the trial site, as reported in the geotechnical section of Figure 2. Table 1 summarizes the basic information of the in-situ tests used for verifying the ground improvement effectiveness. The ground water table (GWT) fluctuations at the trial site results strongly influenced by the tide of the Guayas river, in accordance with the measurements of the tides database INOCAR (2021).



133

134

Table 1. Summary information of the in situ tests at the trial site

Field test	Depth (m)	GWT depth* (m)	Test date
SPTP3_NS	19.0	2.0	2017
CPTu14_NS	20.8	2.7	Feb-18
SDMT1_NS	20.4	3.4	Aug-19
SDMT2_TS	20.6	3.4	Aug-19
CPTu1_NS	17.6	3.8	Aug-20
CPTu2_TS	19.0	3.8	Aug-20

135

\*Note: Measured from the ground surface post filling.

136

137

### 3.2. Geotechnical profile

138

139

140

141

142

143

144

145

146

147

148

149

150

151

152

Figures 2 and 3 summarize the geotechnical profile of the natural soil using borehole and lab testing, SPT, CPTu and SDMT tests (CPTu14\_NS, CPTu1\_NS, SDMT2\_TS and CPTu2\_TS are projected on the cross-section of Figure 2). Beneath the shallow fill, the soil is variable but four clearly defined layers can be observed. The first layer is approximately 2 m thick and varies from silt to clay, as described by the soil behavior index ( $I_c$ ) profile that intercalates between 2.6 and 3.4, by the material index ( $I_D$ ) values that are between 0.2 and 1.1, and by USCS classification (ASTM D2487-11, 2011) that refers to non-organic clays with high plasticity, the fines content FC, estimated using the samples retrieved from borehole SPTP3\_NS varies from 60 to 99%, while the plasticity index (PI) ranges between 42% and 67%. Underlying this layer, loose to medium dense sand mixtures ( $2 \text{ MPa} < q_t < 8 \text{ MPa}$ ;  $2 < K_D < 9$ ,  $5 < (N_1)_{60} < 16$ ) are present until a maximum depth of  $\approx 10$  m. These non-plastic sands and silty sands (SP-SM according to USCS) are mainly characterized by  $I_c < 2.6$  and  $I_D > 1.2$  with FC between 6 and 26%. A lens, of silt mixtures ( $2.6 < I_c < 3.0$ ,  $0.6 < I_D < 1.1$ ) of variable thickness is present within the sandy layer between  $\approx 7$  and 10 m depth. Finally, below 10-11 m depth, normally to moderately overconsolidated clays, according to OCR approximation by Marchetti *et al.* (2001) are encountered (FC  $\approx 67$ -99% and PI  $\approx 43$  - 67%), associating the following DMT and CPTu parameters:  $2.2 < K_D < 3.3$ , with  $3.1 < I_c < 3.9$ ,  $0.2 < q_t < 2.0$  and  $0.2 < I_D < 0.6$ .

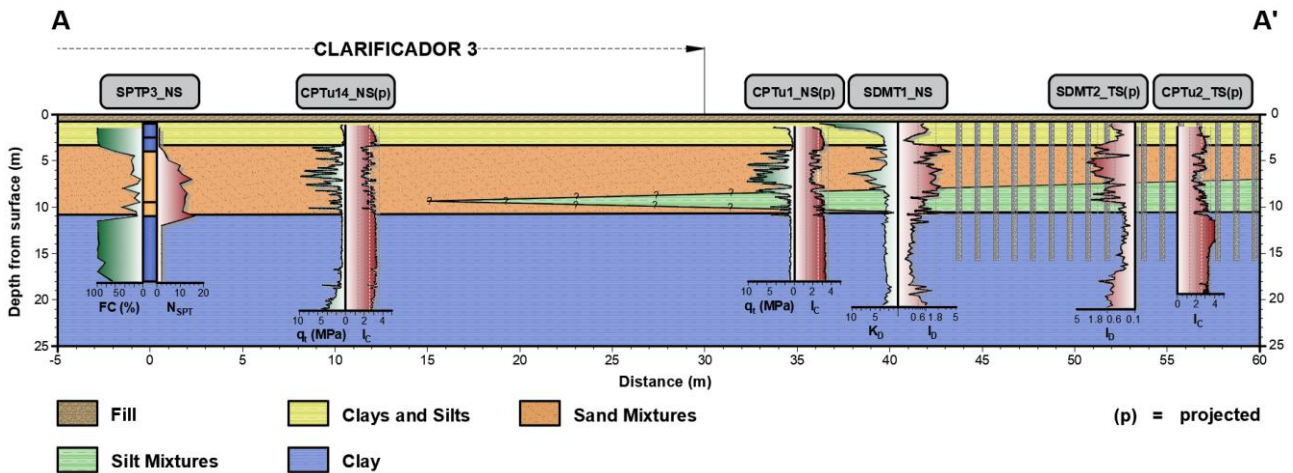


Figure 2. Geotechnical Section

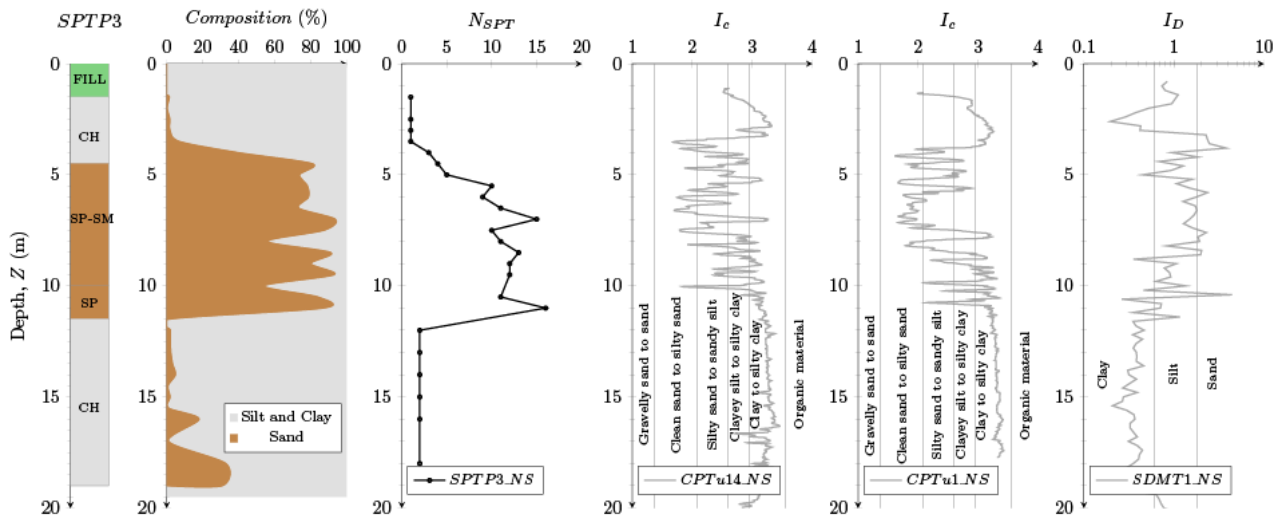


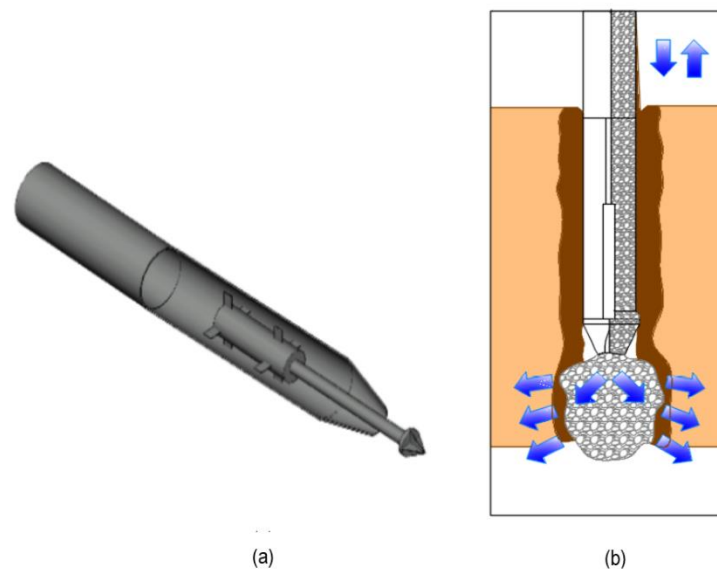
Figure 3. Borehole, FC,  $N_{SPT}$ ,  $I_c$ ,  $I_D$  profiles from in situ tests

### 3.3. Ground improvement

There are two similar vibratory methods to densify the soil: vibro-compaction (also referred as vibroflotation) and vibro-replacement. Both use identical equipment for the installation, but they use different material to fill up the voids generated during the vibration (compaction). Extensive literature agrees that vibro-compaction is more effective for clean sands with low silt content, and the use of sand is recommended to be used as backfill. On the other hand, vibro-replacement is preferable to soils with a higher FC and stone is used instead of sand as backfill (Mitchell and Wentz, 1991; Mitchell, 2008).

The selection of stone columns (SC) built by vibro-replacement as ground improvement method for the project was motivated to counteract the effects of liquefaction in silty sand to sandy silt soils, characterized by soil behavior type index  $I_c < 2.6$  and material index  $I_D > 1.2$ , and to reduce the settlement due to the consolidation of clayey materials (Luque, 2018). In the study area, these deposits are located in a layer between  $\approx 3$  to 10

170 m of depth, overlaying a clay deposit (Figure 3). The 15 m-long and 0.55 m-diameter SC were installed in  
171 different zones of the project area in a staggered arrangement with 2 m-spacing between columns.  
172 For the SC installation by vibro-replacement the primary equipment consists of a vibrating probe with an inner  
173 rotating eccentric mass around the horizontal axis (a scheme is shown in Figure 4(a)), which penetrates the  
174 soil by its self-weight and vibrations. Once it reaches the specified depth, the probe is lifted and the generated  
175 empty space is filled with stone; the probe is lowered to the deposited material to force the stone into the  
176 surrounding soil, forming a stone column (an illustration of this process is shown in Figure 4(b)) (Mackiewicz  
177 and Camp, 2007).



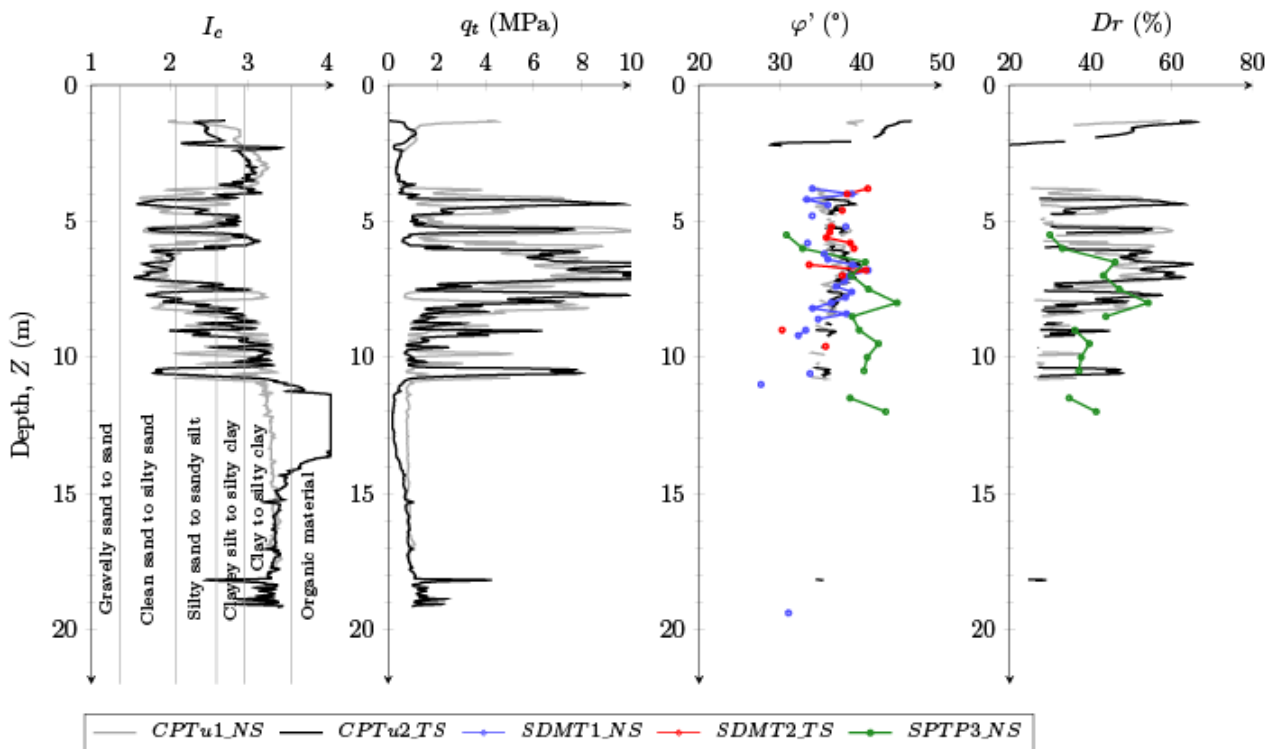
178  
179 Figure 4. (a) Schematic of the vibrating probe. (b) Illustration of the insertion of the vibrating probe and the fill  
180 up of the resulting void with stone  
181

## 182 4. Results

### 183 4.1. Soil improvement

184 Figure 5 shows the variation of the CPTu parameters in natural soil (NS) and treated soil (TS), estimated  
185 according to Robertson and Cabal (2015). The relative density ( $D_R$ ) and the effective friction angle ( $\phi'$ )  
186 estimations are based on the correlations proposed by Kulhawy and Mayne (1990) and Jefferies and Been  
187 (2006) respectively.  $I_c$  profiles present a very slight variability of the soil before and after treatment, which  
188 makes quite comparable the data within the depth of the SC improvement where the silty sand to sandy silt  
189 layer ( $I_c < 2.6$ ) is located. However, for some depth intervals between 4 and 10 m,  $q_t$  ( $\approx 4.2$ -6 m, 8-9 m, 9.6-  
190 10.4 m depth), and  $D_R$  ( $\approx 4.5$ -6 m, 8-9 m depth) values in the NS are somewhat higher than in TS. This is  
191 observed when the  $I_c$  increases in the TS behaving more like a fine grained soil. The  $\phi'$  profile in TS presents  
192 a slight increase throughout the entire  $I_c < 2.6$  layer. Figure 5 also compares the CPTu- $\phi'$  profiles with ones

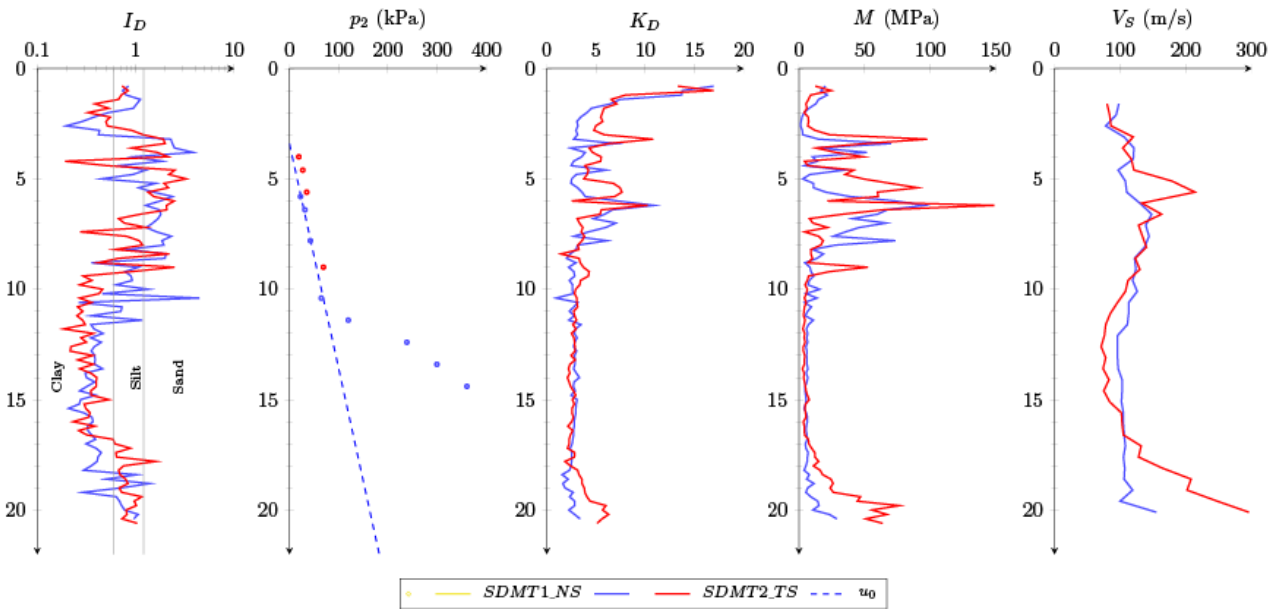
193 estimated from DMT (Marchetti *et al.*, 2001) and SPT (Kulhawy and Mayne, 1990), and the CPTu- $D_R$  values  
 194 with the ones evaluated from SPT (Skempton, 1986); Skempton (1986) tested five types of sand and proposed  
 195 different a and b values for each type of sands,  $D_R$  values are estimated with  $a = 27$ ,  $b = 28$  up to 8.5 m depth,  
 196 from that depth  $a = 38$ ,  $b = 50$  is used. Friction angle ( $\phi'$ ) profiles from DMT and CPTu follow the same trend for  
 197 NS and TS while for the SPT in the NS, the friction angle is overpredicted from  $\approx 7$  to 10 m depth. The  $D_R$  SPT-  
 198 based values in the NS are in good agreement with the related CPTu ones from  $\approx 6$  to 8 m depth, while  
 199 between 8 and 11 m depth, SPT-based method overpredicts the relative density. The SPT-based  
 200 overestimations of  $D_R$  and  $\phi'$  can be attributed to the lens of silt mixtures present detected only by CPTu and  
 201 SDMT located in the proximity of the SC arrangement, while the SPT-based values were measured in the  
 202 layer composed by the sand mixtures.



203  
 204 Figure 5. Results (pre and post treatment)  $I_c$ ,  $q_t$ ,  $\phi'$ ,  $D_R$   
 205

206 Figure 6 presents the plots of the DMT parameters which were calculated using the Marchetti *et al.* (2001)  
 207 formulae. The GWT location was well determined by the equilibrium pore pressure,  $u_0$ , obtained from the third  
 208 DMT pressure reading ( $p_2$ ) into the sandy layers. A certain lateral soil heterogeneity is distinguishable in the  
 209 NS and TS,  $I_D$  profiles between  $\approx 6$  to 8 m depth: the TS exhibits a fine grained soil behavior, considering the  
 210 lower  $I_D$  values ( $0.3 < I_D < 1.2$  corresponding to silty clay to silt), while the NS of the same layer results mostly  
 211 silty-sandy ( $1.2 < I_D < 2.3$ ). This response helps to understand why for the same depth interval the horizontal  
 212 stress index  $K_D$  and the constrained modulus  $M$  are much lower despite the SC installation. The effectiveness

213 of the treatment results then much more noticeable from  $\approx 2$  to 6 m depth, by  $M$  and  $K_D$  profiles. In this depth  
 214 range (2 to 6 m) the  $I_D$  ranges between 0.2 to 3.8 indicating clayey and sandy soils, and  $K_D$  increased 52%  
 215 after treatment. The shear wave velocity  $V_S$  also provides some increase after improvement, but limited  
 216 between 4 and 6 m.



217  
 218 Figure 6. SDMT results (pre and post treatment)  $I_D$ ,  $p_2$ ,  $K_D$ ,  $M$ ,  $V_S$   
 219

220 The analysis of CPTu and DMT combined parameters are displayed in Figure 7 to monitor ground improvement  
 221 effectiveness. The profile of the ratio  $M/q_t$ , which is limited to silty sand to sandy silt soils (i.e.  $I_c < 2.6$  and  $I_D >$   
 222  $1.2$ ) exhibit a 65 % increase after the treatment. The estimation of the over-consolidation ratio OCR and of the  
 223 in-situ earth pressure coefficient  $K_0$  was performed both in fine-grained and incoherent soils. In particular, for  
 224  $I_D < 1.2$  OCR and  $K_0$  were estimated only by DMT using Marchetti *et al.* (2001) formulae, while for sandy layers  
 225 ( $I_c < 2.6$  and  $I_D > 1.2$ ) the combined CPT-DMT approach was used according to Equation 2 from Monaco *et*  
 226 *al.* (2014) for OCR and to Equation 1 from Hossain and Andrus (2016) for  $K_0$ . The OCR and  $K_0$  profiles detect  
 227 the effectiveness of the SC treatment between  $\approx 2.6$  and 6.6 m depth. Below 6.6 m the trend in the NS and TS  
 228 is the same despite the SC installation up to 15 m, due to the presence of the cohesive layer.

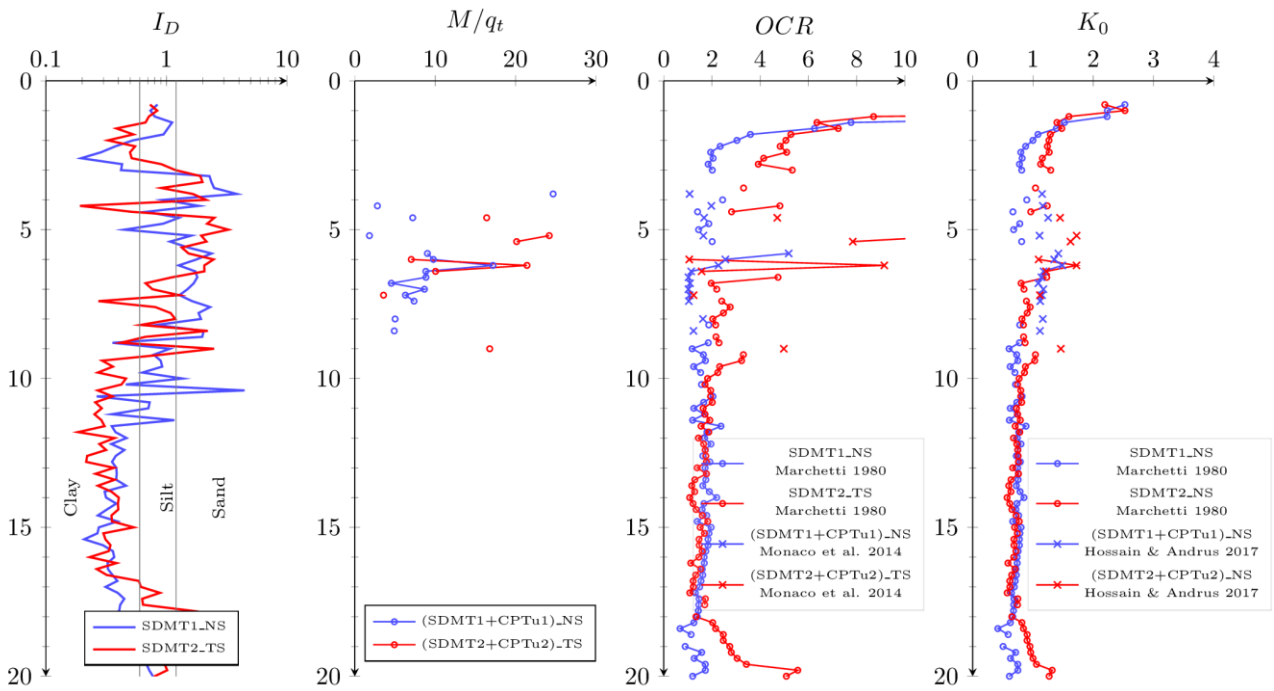


Figure 7. DMT and CPTu combined interpretation (pre and post treatment)  $M/q_t$ , OCR,  $K_0$

229

230

231

232 Table 2 summarizes the average test results of the single and combined parameters from CPTu and SDMT in  
 233 the layer where the increase was better noticed and for  $I_c < 2.6$  and  $I_D > 1.2$ , that is approximately between 3.2  
 234 and 6.6 m depth. The improvement was calculated by relating the difference between TS and NS to NS results,  
 235 expressed as a percentage. The CPTu conventional indicators of improvement show an increment of 6% for  
 236  $q_t$  and 7% for  $D_R$ , while for the SDMT parameters;  $K_D$  increased 22%,  $M$  twice as  $K_D$  and  $V_s$  26%. The  $M/q_t$  ratio  
 237 seems to be more sensitive to the improvement than  $K_D$  and  $M$ , being 65% higher in the TS. For the combined  
 238 CPTu and SDMT parameters,  $K_0$  increased just 15% while OCR increased 98%.

239 Table 2. Summary of average parameters (pre and post treatment) between 3.2 and 6.6 m depth:  $q_t$ ,  $D_R$ ,  $K_D$ ,

240

$M$ ,  $V_s$ ,  $M/q_t$ , OCR,  $K_0$

	$q_t$ (MPa)	$D_R$ (%)	$K_D$	$M$ (Mpa)	$V_s$ (m/s)	$M/q_t$	OCR	$K_0$
NS	5.00	42.49	5.04	43.55	121.20	10.02	3.08	1.27
TS	5.30	45.70	6.17	61.85	152.80	16.54	6.11	1.47
Increase (%)	6.00	7.55	22.42	42.02	26.07	65.06	98.37	15.75

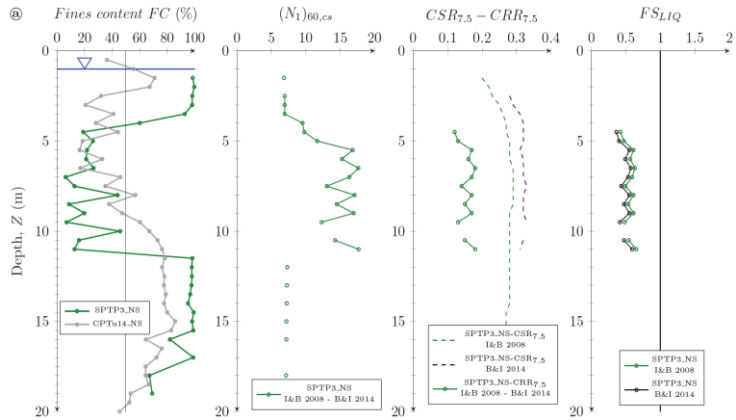
241

242

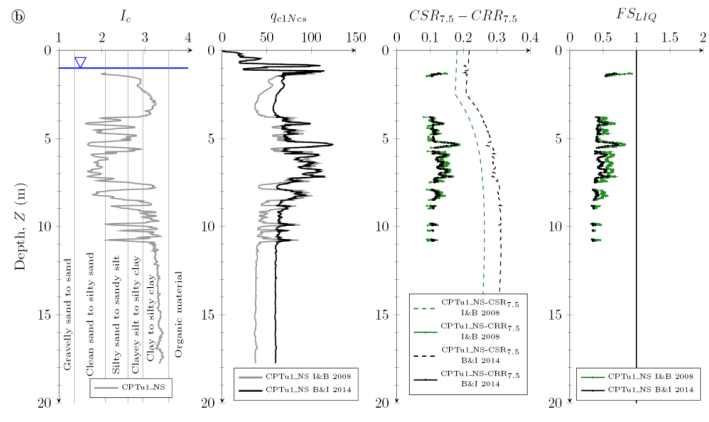
243  
244

4.2. Variation of the liquefaction susceptibility due to the ground improvement

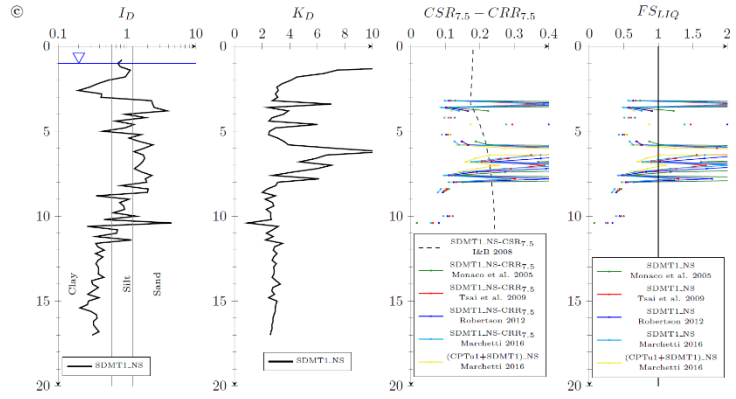
245



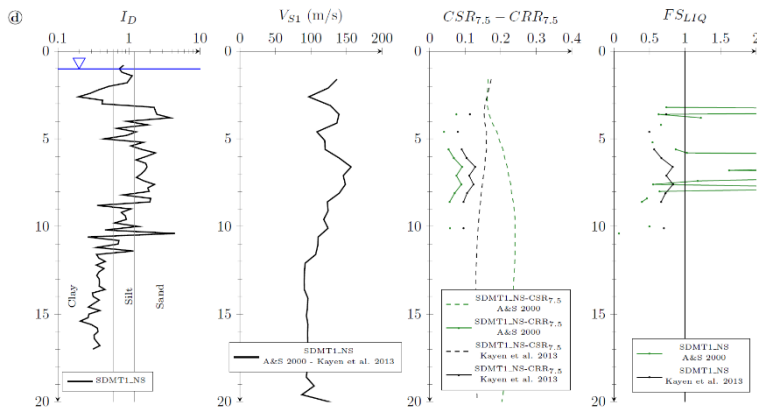
246



247



248

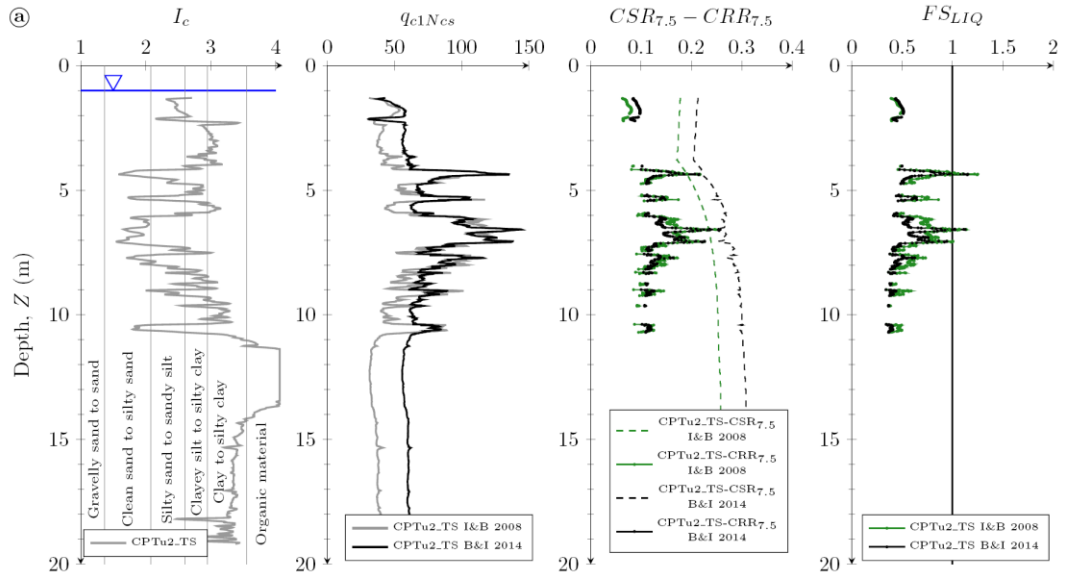


249

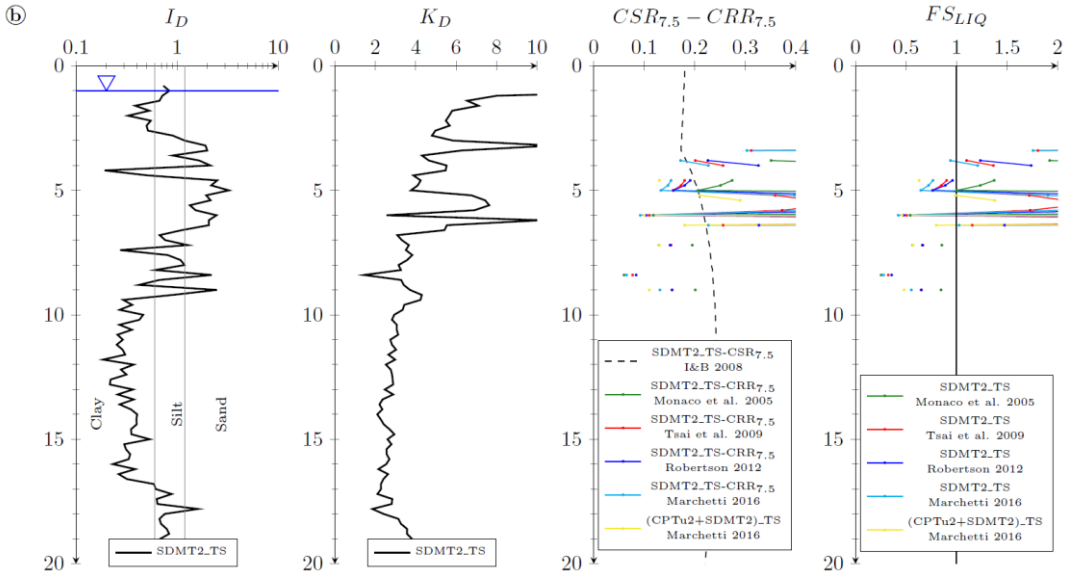
Figure 8. Liquefaction assessment before treatment (NS) for: (a) SPT; (b) CPTu; (c) DMT and CPT+DMT; and (d) Vs methods

250

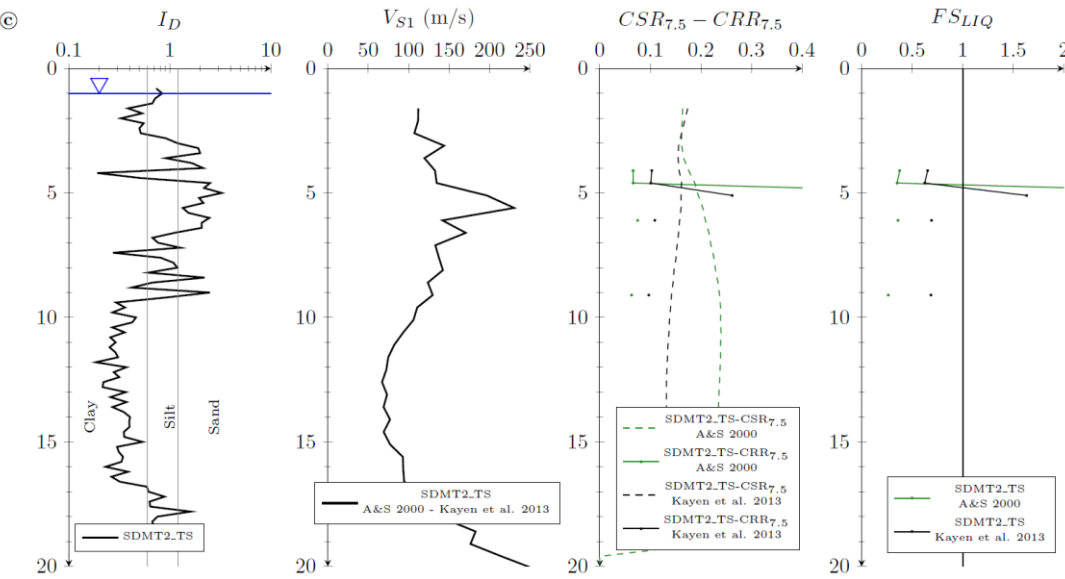
251



252



253



254

Figure 9. Liquefaction assessment after treatment (TS) for: (a) CPTu; (b) DMT and CPT+DMT; and (c) Vs methods

255



256

257 For evaluating the effectiveness of the ground improvement, a liquefaction assessment was performed in  
258 natural and treated soils. The stress-based approach based on the simplified procedure from Seed and Idriss  
259 (1971) was used for the liquefaction analyses, where the cyclic stress ratio at 7.5 magnitude ( $CSR_{M=7.5}$ ) was  
260 obtained according to the ground response analysis performed by Geoestudios (2014). In particular, the design  
261 ground motion of the trial site corresponds to an earthquake with a moment magnitude ( $M_w$ ) equal to 6.7 and  
262 a peak ground acceleration (PGA) of 0.34 g, with the ground water table (GWT) during earthquake assumed  
263 at 1.0 m below the surface level. These values were then used to evaluate  $CSR_{M=7.5}$  based on the simplified  
264 procedure. The magnitude scaling factor (MSF), as well as the shear stress reduction coefficient ( $r_d$ ) were  
265 estimated from Idriss and Boulanger (2008) and Boulanger and Idriss (2014) for the SPT, CPTu and DMT  
266 data; and from Andrus and Stokoe (2000) and Kayen *et al.* (2013) for the  $V_s$  data. The cyclic resistance ratio  
267 ( $CRR_{M=7.5}$ ) was evaluated using correlations with the equivalent clean-sand normalized cone resistance  $(q_{c1N})_{cs}$   
268 and the equivalent clean-sand corrected standard penetration resistance  $(N_1)_{60,cs}$  for the CPTu and SPT data  
269 respectively Idriss and Boulanger (2008), Boulanger and Idriss (2014); with the horizontal stress index  $K_D$  for  
270 the SDMT data Monaco *et al.* (2005), Tsai *et al.* (2009), Robertson (2012), Marchetti (2016); with the  
271 combination of  $(q_{c1N})_{cs}$  and  $K_D$  Marchetti (2016); and with the corrected shear wave velocity  $V_{s1}$  Andrus and  
272 Stokoe (2000), Kayen *et al.* (2013). FC values estimated from correlations with  $I_c$  from CPTu (Suzuki *et al.*,  
273 1998) were used in the CPTu, CPT+DMT and  $V_s$  liquefaction analyses, while FC laboratory measurement  
274 were used into SPT assessment. As shown in Figure 8(a), the two FC profiles results in reasonable agreement,  
275 corroborating the choices of the liquefaction analyses.

276 Before discussing the liquefaction performance indexes on the different methods, it is important to observe  
277 how the different classification and resistance parameters vary with depth before and after treatment (Figure  
278 8 and 9 respectively). For the natural soil, Figure 8(a) shows that for SPT method, there is a liquefiable layer  
279 approximately between 4 and 11 meters of depth, being that in this layer FC is lower than 50% and  $(N_1)_{60,cs}$   
280 lower than 20. Idriss and Boulanger (2008) and Boulanger and Idriss (2014) approaches provide same profiles  
281 of  $(N_1)_{60,cs}$  and  $CRR_{M=7.5}$  while they result slightly different in terms of  $CSR_{M=7.5}$  and hence of  $FS_{LIQ}$ . Figure 8(b)  
282 shows that for CPTu methods, the liquefiable layer is still between around 4 and 11 meters of depth (which  
283 matches well with the SPT method), being  $I_c$  lower than 2.6 and  $(q_{c1N})_{cs}$  lower than 200.  $(q_{c1N})_{cs}$ ,  $CRR_{M=7.5}$  and  
284  $CSR_{M=7.5}$  are different for both methods but they have rather similar  $FS_{LIQ}$  along the liquefiable layer. On the  
285 other hand, Figure 8(c) shows that for DMT method, the liquefiable layer is between around 3 and 11 meters  
286 of depth, being  $I_D$  mostly higher than 1.2 and  $K_D$  mostly lower than 8. There is small difference in  $CRR_{M=7.5}$

287 between the DMT and CPT+DMT methods and consequently in the  $FS_{LIQ}$  profiles. Figure 8(d) shows that for  
288  $V_s$  method, the liquefiable layer is between 3 and 10 meters of depth, corresponding to  $I_D$  mostly higher than  
289 1.2 and  $V_{S1}$  lower than 200 m/s.  $V_{S1}$ ,  $CRR_{M=7.5}$  and  $CSR_{M=7.5}$  are different for both methods (Andrus and Stokoe,  
290 2000; Kayen *et al.*, 2013), resulting in a  $FS_{LIQ}$  lower than 1.

291 As for after treatment results, Figure 9(a) shows no difference in the liquefiable layer thickness for CPTu  
292 assessment as pre-treatment corresponding case, but there are depth intervals (around 4.3 and 6.6 m) where  
293 the  $FS_{LIQ}$  results higher than 1. Figure 9(b) shows a decrease in the liquefiable layer thickness (between 4.5  
294 meters and 9 m of depth), with thicker layers (between 5 and 6.5 m) over the  $FS_{LIQ} = 1$  line than previously  
295 observed. Figure 9(c) also highlights a decrease in the liquefiable layer thickness, limited to few points between  
296 4 and 9 m of depth.

297 The liquefaction potential index (LPI, Iwasaki *et al.*, 1978), the Ishihara-inspired liquefaction potential index  
298 ( $LPI_{ISH}$ , Maurer *et al.*, 2015) which takes into account the thickness of the non-liquefiable capping layer (in this  
299 case  $H_1 = 2.5$ m), the liquefaction severity number (LSN, Tonkin and Taylor, 2013), and the liquefaction-induced  
300 vertical settlement ( $S$ , Zhang *et al.*, 2002) were calculated for all methods before and after ground  
301 improvement, considering the post-liquefaction volumetric strain ( $\epsilon_v$ , Zhang *et al.*, 2002) and the equivalent  
302 clean-sand normalized cone resistance ( $q_{c1N}$ )<sub>cs</sub> from CPTu data. In particular, for the DMT and  $V_s$  methods,  
303 the ( $q_{c1N}$ )<sub>cs</sub> values from CPTu1\_NS were used for the NS and from CPTu2\_TS for the TS, while for the SPT  
304 method, it was necessary to use the ( $q_{c1N}$ )<sub>cs</sub> profile related to CPTu14\_NS. A comparison between these  
305 liquefaction vulnerability indicators calculated before and after ground improvement by SPT, CPTu, DMT,  
306 CPT+DMT and  $V_s$  is presented in Table 3.

307

Mw = 6.7, PGA = 0.34g, GWT = 1m													
Method		LPI (NS)	LPI (TS)	LPI Change (%)	LPI <sub>ISH</sub> (NS)	LPI <sub>ISH</sub> (TS)	LPI <sub>ISH</sub> Change (%)	LSN (NS)	LSN (TS)	LSN Change (%)	S (cm) (NS)	S (cm) (TS)	S Change (%)
SPT	I&B (2008)	18.22	-	-	10.75	-	-	29.81	-	-	14.03	-	-
	B&I (2014)	20.72	-	-	12.21	-	-	29.81	-	-	14.10	-	-
CPT <sub>u</sub>	I&B (2008)	13.46	12.05	10.5	7.96	4.13	48.2	21.35	32.82	-53.7	11.29	11.88	-5.2
	B&I (2014)	16.32	14.47	11.3	9.74	6.12	37.1	22.59	32.15	-42.3	11.83	12.18	-2.9
DMT	Monaco <i>et al.</i> (2005)	6.22	2.00	67.9	3.92	1.02	73.9	15.33	4.60	70.0	8.68	3.81	56.1
	Tsai <i>et al.</i> (2009)	7.77	3.15	59.4	4.70	1.44	69.3	18.50	8.92	51.8	10.45	5.89	43.6
	Robertson (2012)	7.79	3.01	61.4	4.67	1.45	69.0	17.83	7.94	55.5	10.01	5.44	45.6
	Marchetti (2016)	9.70	4.25	56.2	5.90	2.34	60.2	19.08	11.37	40.4	10.78	6.88	36.2
CPT + DMT	Marchetti (2016)	5.38	2.73	49.3	3.01	1.47	51.1	10.32	4.85	53.0	5.95	3.00	49.6
V <sub>s</sub>	A&S (2000)	22.44	9.21	59.0	13.81	6.12	55.7	27.50	12.77	53.6	16.88	6.73	60.1
	Kayen <i>et al.</i> (2013)	10.20	4.75	53.4	5.80	3.21	44.7	27.32	12.93	52.7	16.76	6.82	59.3

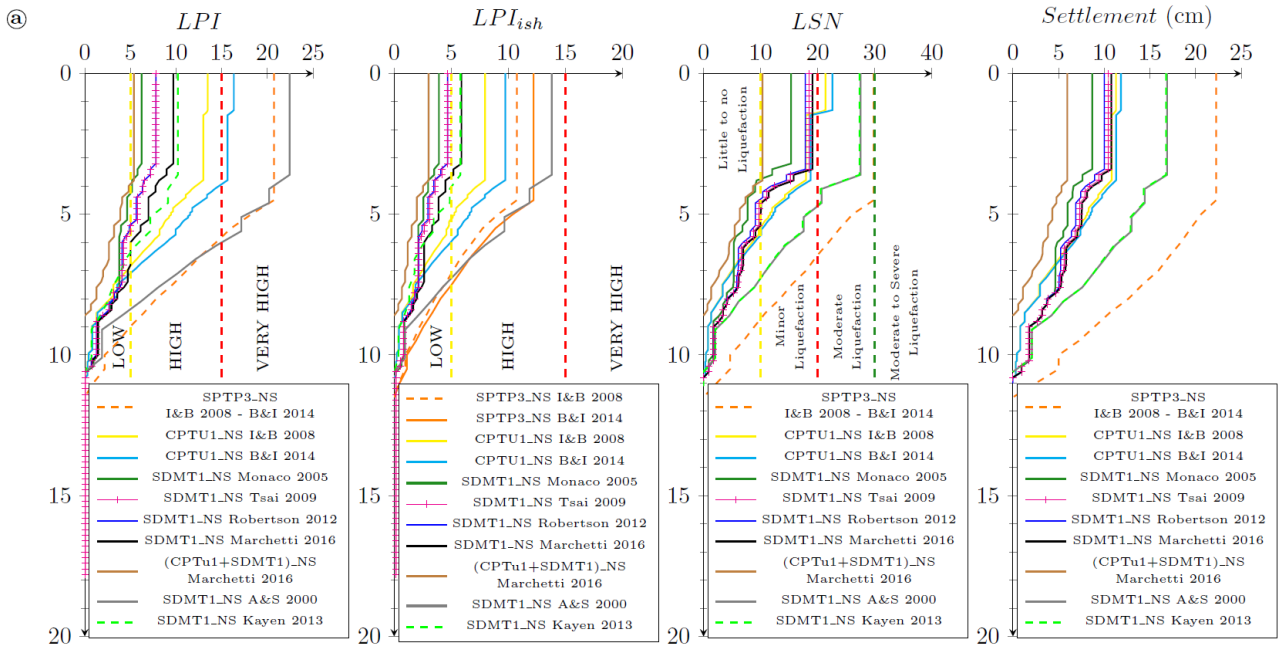
310

311 Figures 10(a) and (b) (before and after treatment) show the different severity liquefaction indicators for all the  
312 methods. In general, all the indexes for the CPT<sub>u</sub> methods seem to provide different results in comparisons  
313 with all the other methods (Figure 10 and Table 3). The change (in percentage) was calculated by the  
314 difference between the treated soil value (TS) and the natural soil value (NS), divided by the NS value (i.e.  
315 positive values correspond to a gain of liquefaction resistance, and negative values indicate a loss of  
316 liquefaction resistance). LPI values from DMT methods show a larger decrement after the ground improvement  
317 (on average from 56% to 68%, moving therefore from high to low liquefaction potential) when compared with  
318 combined CPT+DMT (on average 49%, with LPI values similar to DMT approaches), and V<sub>s</sub> methods (on  
319 average from 53 to 59%, moving from very high to high liquefaction potentials). On the other hand CPT<sub>u</sub>  
320 methods result in a slight decrement in LPI (on average 11%, remaining in the range of high liquefaction  
321 potential). Again, LPI<sub>ISH</sub> values from DMT methods apparently provide a larger decrement (on average from

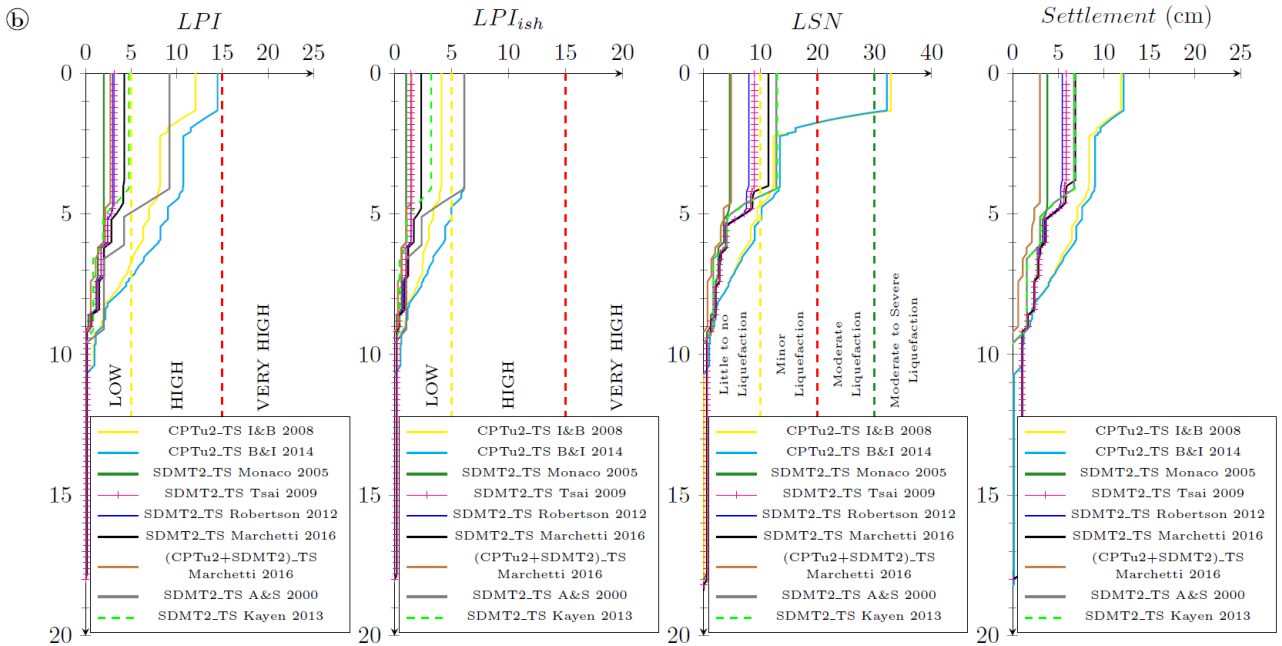
322 60 to 74%, reaching  $LPI_{ISH} \approx 1-2$  after treatment) when compared with CPTu methods (on average from 37 to  
323 48%, reaching moderate and barely to high liquefaction potential), combined CPT+DMT (on average 51%,  
324 with LPI values similar to DMT approaches), and  $V_s$  methods (on average from 45 to 56%, detecting however  
325 after pier installations higher LPI  $\approx 3-6$ ). LSN decreases are very similar for all the methods (on average from  
326 53 to 70%), except for the CPTu methods, which actually result in an increment in LSN (on average from -42%  
327 to -54%, corresponding to moderate to severe liquefaction after the treatment). However LSN absolute values  
328 from  $V_s$  approaches are generally higher than the ones obtained from DMT and CPT+DMT methods, moving  
329 from moderate (NS) to minor liquefaction (TS). For the settlement (S), the  $V_s$  methods show the larger  
330 decrement for before and after the ground improvement (on average 60%) compared to both DMT and  
331 combined CPT+DMT methods (on average from 36 to 56%). However, all these methods show that S varies  
332 approximately between 6 and 17 cm in NS and between 3 and 7 cm in TS. As with LPI and LSN values, CPTu  
333 methods result in a slight increase in settlement after the ground improvement (on average from -3 to -5%, or  
334 basically no change in settlement). Since SPT tests were performed at the site only on natural soil, there is no  
335 comparison between natural and treated soils for this method, but the liquefaction severity indexes were  
336 calculated before the improvement, resulting in a reasonable agreement with DMT, CPT+DMT, and  $V_s$   
337 methods. The inconsistencies of CPTu liquefaction results may be mostly due to the small increase of CPTu  
338 parameters after the SC installation (see Table 2), nevertheless the  $I_c$  profiles are quite similar before and after  
339 treatment. Some further small differences may be related to the presence of a shallow liquefiable layer into  
340 CPTu profiles (depth interval  $\approx 1-2$  m), and to a soil lateral variability that reduces the thickness of the silty-  
341 sandy layer only for the SDMT2\_TS test that was performed after treatment.

342

343



344



345

Figure 10. Liquefaction vulnerability indicators: (a) before and (b) after treatment for all methods

346

347 **5. Conclusions**

348 Despite the length of the SCs, the effectiveness of the treatment resulted noticeable only between 3.2 to 6.6  
 349 m depth, where the sand mixtures were detected by in situ tests. Below this layer a lens of silt mixtures, with  
 350 higher FC (up to 46%) approximately between 7 to 10 m depth, and of a cohesive soil layer, from 10-11 m  
 351 depth, were identified.

352 The evaluation of the soil improvement between 3.2 to 6.6 m depth was mainly detected through the use of  
 353 the combined CPTu and SDMT parameters, with a 65% increment in  $M/q_t$ , 98 % increment in OCR and 15%  
 354 increment in  $K_0$ . The relatively low increment in  $K_0$  can be attributed to the high initial  $K_0$  condition in NS  $\approx 1.27$ ,

355 as noticed by Schmertmann (1985). In the CPTu based effectiveness assessment,  $q_t$  and  $D_R$  have a similar  
356 increase (6% and 7.5% respectively), although the NS and TS were related to quite homogeneous subsoil, as  
357 detectable looking at  $I_c$ . On the other hand, SDMT single parameters,  $K_b$ ,  $M$ ,  $V_s$ , provided a more evident SC  
358 improvement, even still limited, of 22%, 42% and 26% respectively.

359 As for liquefaction susceptibility the DMT, CPT+DMT and  $V_s$  analyses showed a higher sensitivity to the  
360 improvement when compared to the CPTu results. On average, the percentage of LPI,  $LPI_{ISH}$ , LSN, and S  
361 improvement for these DMT, CPT+DMT and  $V_s$  methods are equal to 49-68%, 51-74%, 40-70%, and 36-60%,  
362 respectively, while for CPTu they are equal to 10-11%, 37-48%, -42-(-54) %, and -3-(-5)%, respectively. The  
363 inconsistencies of CPTu liquefaction results may be mostly due to the small increase of CPTu parameters after  
364 the SC installation. SPT, CPTu and  $V_s$ , often result in higher absolute values than the other methods (DMT  
365 and CPT+DMT). Overall, SC implementation as ground improvement technique clearly shows a gain in  
366 liquefaction resistance that is better reflected by the DMT, CPT+DMT and  $V_s$  methods.

## 367 6. References

368

- 369 Adalier K and Elgamal A (2004) Mitigation of liquefaction and associated ground deformations by stone  
370 columns. *Engineering Geology*. **72 (3-4)**: 275–291, <https://doi.org/10.1016/j.enggeo.2003.11.001>.
- 371 Amoroso S, Rollins K, Monaco P, Holtrigter M, and Thorp A (2018) Monitoring ground improvement using the  
372 seismic dilatometer in Christchurch, New Zealand. *Geotechnical Testing Journal*. **41 (5)**: 946–966,  
373 <https://doi.org/10.1520/GTJ20170376>.
- 374 Andrus R and Stokoe K (2000) Liquefaction resistance of soils from shear-wave velocity. *Journal of*  
375 *Geotechnical and Geoenvironmental Engineering* **126 (11)**: 1015–1025,  
376 [https://doi.org/10.1061/\(ASCE\)1090-0241\(2000\)126:11\(1015\)](https://doi.org/10.1061/(ASCE)1090-0241(2000)126:11(1015)).
- 377 Baez J (1995) *A Design Model for the Reduction of Soil Liquefaction by Vibro-Stone Columns*, Doctoral thesis,  
378 University of Southern California. University of Southern California, Los Angeles, United States.
- 379 Bałachowski L and Kurek N (2015) Vibroflotation Control of Sandy Soils Using DMT and CPTU. *Proceedings*  
380 *of the 3rd International Conference on the Flat Dilatometer (DMT'15), Rome, Italy* (Marchetti S (ed.)).  
381 ISSMGE TC 102, p. 6.
- 382 Baldi G, Belloti R, Ghioma N and Jamiolkowski M (1988) Stiffness of sands from CPT, SPT, DMT — A critical  
383 review. *Penetration testing in the UK*. (Thomas Telford Publishing), pp. 299–305.  
384 <https://doi.org/10.1680/ptituk.13773.0051>

385 Baldi G, Belloti R, Ghioma V, Jamiolkowski M, Marchetti S and Pasqualini E. (1986) Flat Dilatometer Tests in  
386 Calibration Chambers. *Proceedings In Situ '86 ASCE Specialty Conference on Use of In Situ Tests in*  
387 *Geotechnical Engineering*. Virginia Tech, Blacksburg, VA. ASCE Geot. Special Publ. No. 6. pp. 431–  
388 446.

389 Boulanger R and Idriss I (2014). CPT and SPT based liquefaction triggering procedures. *Report No.*  
390 *UCD/CGM.-14, 1*, p. 134.

391 Hossain A and Andrus R (2016) At-Rest Lateral Stress Coefficient in Sands from Common Field Methods.  
392 *Journal of Geotechnical and Geoenvironmental Engineering*. **142 (12)**: 1–5,  
393 [https://doi.org/10.1061/\(ASCE\)GT.1943-5606.0001560](https://doi.org/10.1061/(ASCE)GT.1943-5606.0001560).

394 Idriss I and Boulanger R (2008) Soil liquefaction during earthquakes. Earthquake Engineering Research  
395 Institute, Oakland, CA, *EERI Report No. MNO-12*, p.237.

396 INOCAR (2021) Instituto Oceanográfico y Antártico de la Armada - Tabla de mareas puertos del Ecuador  
397 (Oceanographic and Antarctic Institute of the Navy - Table of tides of ports of Ecuador) . See  
398 <https://www.inocar.mil.ec/web/index.php/productos/tabla-mareas#busqueda-de-datos-de-mareas>  
399 (accessed 2021 Mar 22].

400 Iwasaki T, Tatsuoka F, Tokida K, Yasuda S (1978). A practical method for assessing soil liquefaction potential  
401 based on case studies at various sites in Japan. *Proceedings Second International Conference on*  
402 *Microzonification Safer Construction Research Application*. Vol. 2 pp. 885–896

403 Jefferies M and Been K (2006) Soil liquefaction—A critical state approach. Taylor and Francis, p. 478.

404 Jendebly L (1992) Deep Compaction by Vibrowing. *Proceedings of Nordic Geotechnical Meeting NGM-92*,  
405 Aalborg, Denmark, Danish Geotechnical Society, Lyngby, Denmark, pp. 19–24.

406 Juang C, Huang X, Holtz R and Chen J (1996) *Determining relative density of sands from CPT using fuzzy*  
407 *sets*. *Journal of Geotechnical Engineering*. **122 (1)**:1–6, [https://doi.org/10.1061/\(ASCE\)0733-](https://doi.org/10.1061/(ASCE)0733-9410(1996)122:1(1))  
408 [9410\(1996\)122:1\(1\)](https://doi.org/10.1061/(ASCE)0733-9410(1996)122:1(1)).

409 Kayen R, Moss R, Thompson E, et al. (2013) Shear-Wave Velocity-Based Probabilistic and Deterministic  
410 Assessment of Seismic Soil Liquefaction Potential. *Journal of Geotechnical and Geoenvironmental*  
411 *Engineering* **139 (3)**: 407–419. [https://doi.org/10.1061/\(ASCE\)GT.1943-5606.0000743](https://doi.org/10.1061/(ASCE)GT.1943-5606.0000743).

412 Knappett J and Craig R. (2012) Craig's Soil Mechanics, Eighth Edition. London and New York: Spon Press  
413 pp. 91–96

414 Kulhawey F and Mayne P (1990). Manual on estimating soil properties for foundation design. (No. *EPRI-EL-*  
415 *6800*). Electric Power Research Inst., Palo Alto, CA (USA); Cornell Univ., Ithaca, NY (USA).

416 Geotechnical Engineering Group.

417 Kurek N and Bałachowski L (2015) CPTU/DMT Control of Heavy Tamping Compaction of Sands. *Proceedings*  
418 *of 3rd International Conference on the Flat Dilatometer (DMT'15), Rome, Italy.* (Marchetti S (ed.)).  
419 ISSMGE TC 102, p. 6.

420 Lee M, Choi S, Kim M and Lee W (2011) Effect of stress history on CPT and DMT results in sand. *Journal of*  
421 *Engineering Geology.* **117 (3–4):** 259–265. <https://doi.org/10.1016/j.enggeo.2010.11.005>.

422 Luehring R, Snorteland N, Stevens M and Mejia L (2001) Liquefaction Mitigation of a Silty Dam Foundation  
423 Using Vibro-Stone Columns and Drainage Wicks: A Case History at Salmon Lake Dam. *Water Oper.*  
424 *Manage. Bull.* **(198):** 1–15

425 Luque R (2018) Informe de columnas de grava en zona de estrato tipico 1: suelo arenoso. Proyecto : Planta  
426 de Tratamiento de Aguas Residuales. (report of stone columns in the zone of typical stratum 1: sandy  
427 soils. Project: wastewater treatment plant) p. 34.

428 Mackiewicz S and Camp W (2007) Ground Modification: How Much Improvement? *Geo-Denver 2007, Denver,*  
429 *Colorado, United States,* p.9. [https://doi.org/10.1061/40916\(235\)14](https://doi.org/10.1061/40916(235)14).

430 Marchetti S, Monaco P, Totani G and Calabrese M (2001) The Flat Dilatometer Test (DMT) in Soil  
431 Investigations— A Report by the ISSMGE Committee TC16. *Proceedings of In Situ 2001, International*  
432 *Conference on In Situ Measurement of Soil Properties, Bali, Indonesia.* ISSMGE, London, UK, p.42.

433 Marchetti D, Marchetti S, Monaco P and Totani G (2008). Experience with seismic dilatometer ( SDMT ) in  
434 various soil types. *Geotechnical and Geophysical Site Characterization 2:* 1339–1345.

435 Marchetti S (1980) In Situ Tests by Flat Dilatometer. *Journal of Geotechnical Engineering Division* **106 (3):**  
436 299–321.

437 Marchetti S. (2016) Incorporating the Stress History Parameter  $K_D$  of DMT into the Liquefaction Correlations  
438 in Clean Uncemented Sands. *Journal of Geotechnical and Geoenvironmental Engineering* **142 (2):**  
439 04015072. [https://doi.org/10.1061/\(ASCE\)GT.1943-5606.0001380](https://doi.org/10.1061/(ASCE)GT.1943-5606.0001380).

440 Massarsch K and Fellenius B (2019) Evaluation of vibratory compaction by in situ tests. *Journal of*  
441 *Geotechnical and Geoenvironmental Engineering* **145 (12):**1–15.  
442 [https://doi.org/10.1061/\(ASCE\)GT.1943-5606.0002166](https://doi.org/10.1061/(ASCE)GT.1943-5606.0002166).

443 Massarsch K and Fellenius B (2002). Vibratory compaction of coarse-grained soils. *Canadian Geotechnical*  
444 *Journal* **39 (3):**695–709. <https://doi.org/10.1139/t02-006>

445 Massarsch K, Wersäll C and Fellenius B (2020). Horizontal stress increase induced by deep vibratory  
446 compaction. *Proceedings of the Institution of Civil Engineers - Geotechnical Engineering.* **173 (3):** 228–



447 253. <https://doi.org/10.1680/jgeen.19.00040>.

448 Maurer B, Green R and Taylor O (2015) Moving towards an improved index for assessing liquefaction hazard:  
449 Lessons from historical data. *Soils and Foundations*. **55 (4)**:778–787.  
450 <https://doi.org/10.1016/j.sandf.2015.06.010>.

451 Mayne P and Kulhawy F (1982)  $K_0$ -OCR Relationship in Soil. *Journal of the Geotechnical Engineering*  
452 *Division*. **108 (GT6)**: 851–872. <http://dx.doi.org/10.1061/AJGEB6.0001306>.

453 Mitchell J and Wentz F (1991) Performance of Improved ground During the Loma Prieta Earthquake. Report  
454 No. *UCB/EERC-91/12*, Earthquake Engineering Research Center, University of California, Berkeley, p.  
455 100.

456 Mitchell J (2008) Mitigation of liquefaction potential of silty sands. *Symposium Honoring Dr John H*  
457 *Schmertmann for His Contributions to Civil Engineering at Research to Practice in Geotechnical*  
458 *Engineering*. New Orleans, Louisiana, United States, pp. 433–451.  
459 [https://doi.org/10.1061/40962\(325\)15](https://doi.org/10.1061/40962(325)15).

460 Monaco P, Amoroso S, Marchetti S, et al. (2014) Overconsolidation and Stiffness of Venice Lagoon Sands  
461 and Silts from SDMT and CPTU. *Journal of Geotechnical and Geoenvironmental Engineering* **140 (1)**:  
462 215–227. [https://doi.org/10.1061/\(ASCE\)GT.1943-5606.0000965](https://doi.org/10.1061/(ASCE)GT.1943-5606.0000965)

463 Monaco P, Marchetti S, Totani G and Calabrese M (2005) Sand Liquefiability Assessment by Flat Dilatometer  
464 Test (DMT). *16th International Conference on Soil Mechanics and Geotechnical Engineering*. Osaka,  
465 Japan: International Society of Soil Mechanics and Geotechnical Engineering, London, UK, pp. 2693–  
466 2697.

467 Rayamajhi D, Ashford S, Boulanger R and Elgamal A (2016) Dense granular columns in liquefiable ground. I:  
468 Shear reinforcement and cyclic stress ratio reduction. *Journal of Geotechnical and Geoenvironmental*  
469 *Engineering* **142 (7)**: 1–11, [https://doi.org/10.1061/\(ASCE\)GT.1943-5606.0001474](https://doi.org/10.1061/(ASCE)GT.1943-5606.0001474).

470 Robertson P and Cabal K (2015) Guide to Cone Penetration Testing for Geotechnical Engineering. 6th ed,  
471 Gregg Drilling and Testing, Signal Hill, CA, p. 131

472 Robertson P (2012) The James K. Mitchell Lecture: Interpretation of In-Situ Tests-Some Insights. *4th*  
473 *International Conference on Geotechnical and Geophysical Site Characterization*. Porto de Galinhas,  
474 Brazil, Taylor and Francis Group, London, England, pp. 3–24.

475 Schmertmann J, Baker W, Gupta R and Kessler K (1986) CPT/DMT quality control of ground modification at  
476 a power plant. *Specialty Conference-In Situ '86*, Virginia Tech, Blacksburg, VA, American Society of  
477 Civil Engineers, Reston, VA, pp. 985–1001.

478 Schmertmann J (1985) Measure and Use of the In Situ Lateral Stress. *Practice of Foundation Engineering. A*  
479 *Volume Honoring Jorj O. Osterberg*. The Department of Civil Engineering, Northwestern University, pp.  
480 189–213.

481 Seed B and Idriss I (1971) Simplified Procedure for Evaluating Soil Liquefaction Potential. *Journal of Soil*  
482 *Mechanics Foundation Division* **97 (9)**: 1249–1273, <https://doi.org/10.1061/JSFEAQ.0001662>.

483 Shenthan T, Thevanayagam S and Martin G (2004) Densification of Saturated Silty Soils Using Composite  
484 Stone Columns for Liquefaction Mitigation. *Proceedings, 13 th World Conference on Earthquake*  
485 *Engineering* Vancouver, B.C., Canada. Paper No. 1930, p. 13.

486 Skempton A (1986) Standard penetration test procedures and the effects in sands of overburden pressure,  
487 relative density, particle size, aging and overconsolidation. *Géotechnique*. **36 (3)**:425–447.  
488 <https://doi.org/10.1680/geot.1986.36.3.425>

489 Suzuki Y, Sanematsu T and Tokimatsu K (1998) Correlation between SPT and seismic CPT. *Geotechnical*  
490 *Site Characterization*, (Proc. ISC'98, Atlanta), Balkema, Rotterdam, Vol. 2, pp. 1375–1380.

491 Tonkin and Taylor. (2013) *Liquefaction Vulnerability Study, Report to Earthquake Commission. Wellington,*  
492 *New Zealand*, p. 50..

493 Tsai P and Lee D, Kung G and Juang C (2009). Simplified DMT-Based Methods for Evaluating Liquefaction  
494 Resistance of Soils. *Eng. Geol.* **103 (2)**:13–22. <https://doi.org/10.1016/j.enggeo.2008.07.008>.

495 U.S. Army Corps of Engineers (1999) Guidelines on Ground Improvement for Structures and Facilities. ETL  
496 1110-1-185. (accessed 2020 Oct 6). See [http://usacetechnicalletters.tpub.com/ETL-1110-1-185/ETL-](http://usacetechnicalletters.tpub.com/ETL-1110-1-185/ETL-1110-1-1850002.htm)  
497 [1110-1-1850002.htm](http://usacetechnicalletters.tpub.com/ETL-1110-1-1850002.htm)

498 Zhang G, Robertson P and Brachman R (2002). Estimating Liquefaction Induced Ground Settlements from  
499 CPT for Level Ground. *Canadian Geotechnical Journal* **39 (5)**:1168–1180. [https://doi.org/10.1139/t02-](https://doi.org/10.1139/t02-047)  
500 047

501

502